

# Numerical Modeling of NBI-Driven Sub-Cyclotron Frequency Modes in NSTX

E. V. Belova (PPPL)

In collaboration with: N. N. Gorelenkov and E. D. Fredrickson



# Motivation

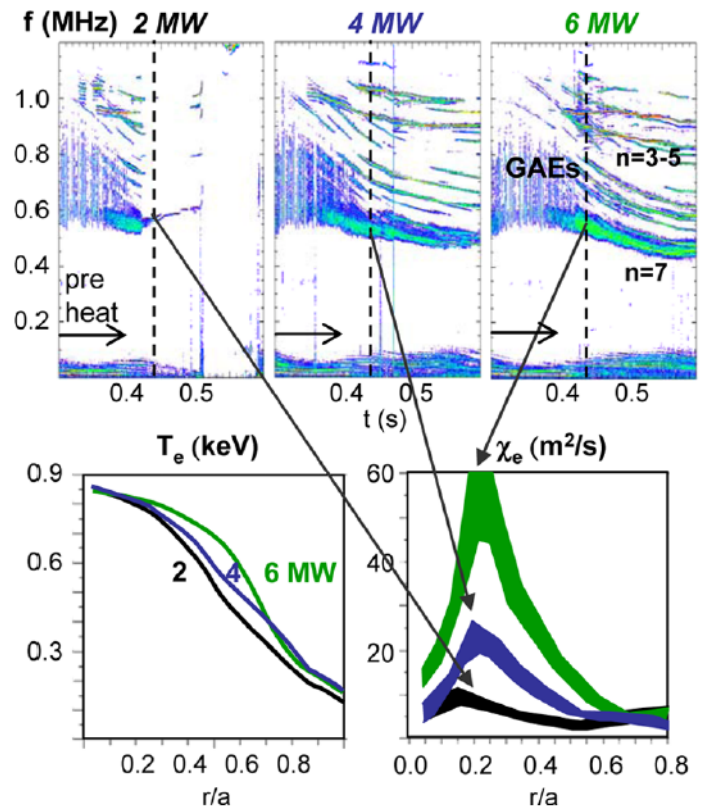
---

---

- Many sub-cyclotron frequency modes are observed in NSTX during NBI injection. These modes were identified as Compressional Alfvén Eigenmodes (CAEs) and Global Alfvén Eigenmodes (GAEs).
- CAE and GAE modes are predicted to be driven unstable by super-Alfvénic NBI ions with  $V_b \sim 3V_A$  (90 keV) through the Doppler shifted cyclotron resonance.
- GAE and CAE modes are capable of channeling the beam ion energy into the thermal ions, they can also induce redistribution of beam ions and strong anomalous electron transport in STs.
- Numerical simulations include: self-consistent anisotropic equilibrium, fully kinetic ion description and nonlinear effects.

# Correlation between strong GAE activity and enhanced electron transport has been observed in NSTX [Stutman, PRL 2009]

- Plasmas with rapid central electron transport show intense GAE activity (0.5-1.1MHz), while low-transport plasmas are GAE free.
- Flattening of the electron temperature profile with increased beam power.
- Correlation is also observed in experiments with the beam energy scanned between 60keV and 90 keV [Stutman, PRL 2009].
- GAE frequencies are comparable with the trapped electron bounce frequency.
- Measurements of GAE amplitude confirm the central localization of the modes [Tritz, APS 2010].
- Test particle simulations using the ORBIT code predict thermal electron transport due to orbit stochasticity in the presence of multiple core localized GAE modes [Gorelenkov, NF 2010].
- Anomalous electron transport potentially can have significant implications for future fusion devices, especially low aspect ratio tokamaks.



Correlation between GAE activity,  $T_e$  flattening, and central electron heat diffusivity  $\chi_e$  in NSTX H modes with 2, 4, and 6MW neutral beam.

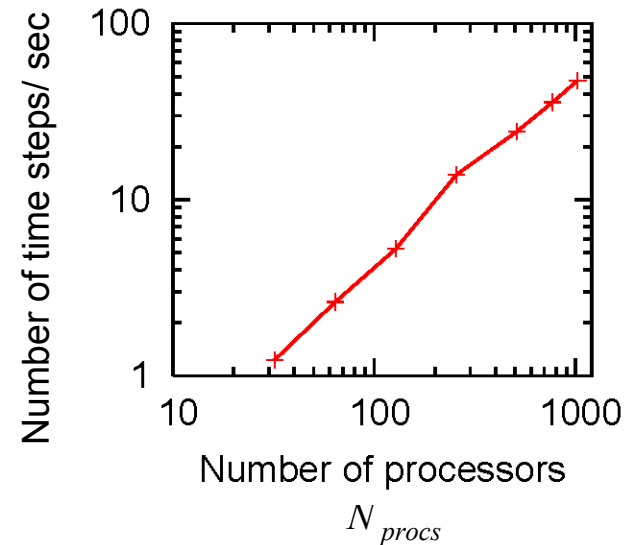
# HYM – Parallel Hybrid/MHD Code

HYM code developed at PPPL and used to investigate kinetic effects on MHD modes in toroidal geometry (FRCs and NSTX)

- 3-D nonlinear.
- Several different physical models:
  - Resistive MHD & Hall-MHD.
  - Hybrid (fluid electrons, particle ions).
  - MHD/particle (one-fluid thermal plasma, + energetic particle ions).
- Full-orbit kinetic ions.
- Drift-kinetic electrons.
- For particles: delta-f / full-f numerical scheme.
- Parallel (3D domain decomposition, MPI)<sup>1</sup>.

<sup>1</sup>Simulations are performed at NERSC.

Parallel scaling MHD run 513x127x32



MPI version of HYM code shows very good parallel scaling up to 1000 processors for production-size simulation runs, and allows high-resolution nonlinear simulations.

# Self-consistent MHD + fast ions coupling scheme

Background plasma - fluid:

$$\rho \frac{d\mathbf{V}}{dt} = -\nabla p + (\mathbf{j} - \mathbf{j}_i) \times \mathbf{B} - n_i (\mathbf{E} - \eta \mathbf{j})$$

$$\mathbf{E} = -\mathbf{V} \times \mathbf{B} + \eta \mathbf{j}$$

$$\mathbf{B} = \mathbf{B}_0 + \nabla \times \mathbf{A}$$

$$\partial \mathbf{A} / \partial t = -\mathbf{E}$$

$$\mathbf{j} = \nabla \times \mathbf{B}$$

$$\partial p^{1/\gamma} / \partial t = -\nabla \cdot (\mathbf{V} p^{1/\gamma})$$

$$\partial \rho / \partial t = -\nabla \cdot (\mathbf{V} \rho)$$

Fast ions – delta-F scheme:

$$\frac{d\mathbf{x}}{dt} = \mathbf{v}$$

$$\frac{d\mathbf{v}}{dt} = \mathbf{E} - \eta \mathbf{j} + \mathbf{v} \times \mathbf{B}$$

$w = \delta F / F$  - particle weight

$$\frac{dw}{dt} = -(1-w) \frac{d(\ln F_0)}{dt}$$

$$F_0 = F_0(\varepsilon, \mu, p_\phi)$$

$\rho$ ,  $\mathbf{V}$  and  $p$  are bulk plasma density, velocity and pressure,  $n_i$  and  $\mathbf{j}_i$  are fast ion density and current,  $n_i \ll n$  – is assumed.

# Self-consistent anisotropic equilibrium including the NBI ions

Grad-Shafranov equation for two-component plasma: MHD plasma (thermal) and fast ions [Belova et al, Phys. Plasmas 2003]

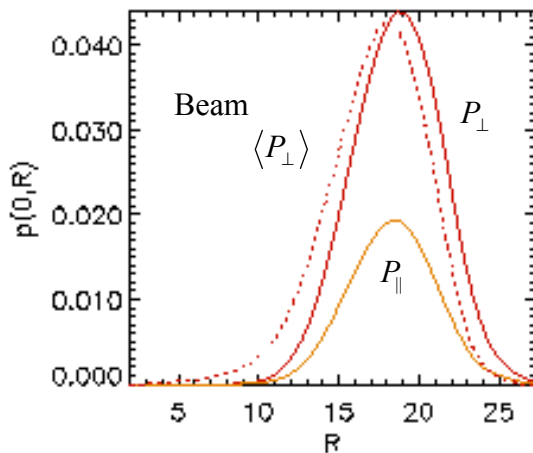
$$\frac{\partial^2 \psi}{\partial z^2} + R \frac{\partial}{\partial R} \left( \frac{1}{R} \frac{\partial \psi}{\partial R} \right) = -R^2 p' - HH' - GH' + RJ_{i\phi}$$

$$\mathbf{B} = \nabla \phi \times \nabla \psi + h \nabla \phi$$

$$h(R, z) = H(\psi) + G(R, z)$$

$$\mathbf{J}_{ip} = \nabla G \times \nabla \phi, \quad G - \text{poloidal stream function}$$

**Fast ions** – delta-f scheme:  $F_0 = F_0(\epsilon, \mu, p_\phi)$ , where  $\mu$  is calculated up to 1<sup>st</sup> order in  $\rho_i / L$ ;  $F_0$  is chosen to match the distribution functions computed from the TRANSP code (L-mode discharges).



The prompt-loss condition, anisotropy, the large Larmor radius of the beam ions and the strong pitch-angle scattering at low energies have been included in order to match the distribution functions computed from the TRANSP code.

Strong modifications of equilibrium profiles due to beam ions: more peaked current profile, anisotropic pressure, increase in Shafranov shift – indirect effect on stability.

# Equilibrium calculations

Equilibrium distribution function  $F_0 = F_1(v)F_2(\lambda)F_3(p_\phi)$

$$F_1(v) = \frac{1}{v^3 + v_*^3}, \quad \text{for } v < v_0$$

$$F_2(\lambda) = \exp(-(\lambda - \lambda_0)^2 / \Delta\lambda^2)$$

$$F_3(p_\phi) = \frac{(p_\phi - p_0)^\beta}{(R_0 v - \psi_0 - p_0)^\beta}, \quad \text{for } p_\phi > p_0$$

where  $v_0 \approx 3v_A$ ,  $v_* = v_0/\sqrt{3}$ ,  $\lambda = \mu B_0/\varepsilon$  - pitch angle,  
 $\lambda_0 = 0.8 - 1$ ,

and  $\mu = \mu_0 + \mu_1$  includes first-order corrections [Littlejohn'81]:

$$\mu = \frac{(\mathbf{v}_\perp - \mathbf{v}_d)^2}{2B} - \frac{\mu_0 v_\parallel}{2B} [\hat{\mathbf{b}} \cdot \nabla \times \hat{\mathbf{b}} - 2(\hat{\mathbf{a}} \cdot \nabla \hat{\mathbf{b}}) \cdot \hat{\mathbf{c}}]$$

$\mathbf{v}_d$  is magnetic gradient and curvature drift velocity,  $\hat{\mathbf{c}} = \mathbf{v}_\perp/v_\perp$ ,  
 $\hat{\mathbf{a}} = \hat{\mathbf{b}} \times \hat{\mathbf{c}}$

# 3D simulations of energetic ion-driven instabilities in NSTX

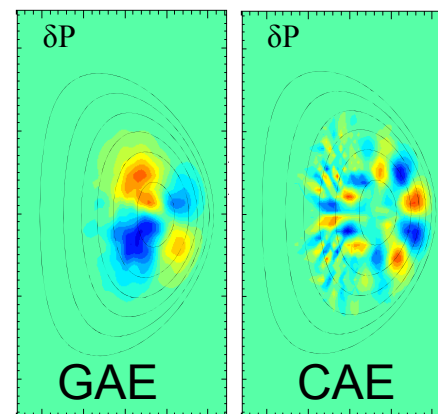
## Linearized delta-f simulations

- Low-n simulations show instability of Global Alfvén Eigenmode (GAE) with large  $k_{\parallel}$ , and significant compressional component.

For  $n=4-9$  :  $\gamma = (0.005 \text{ -- } 0.016)\omega_{ci}$  and  $\omega = 0.2-0.5 \omega_{ci}$

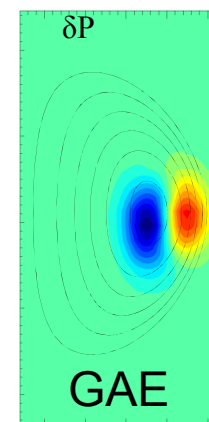
- Simulation with larger n ( $n \geq 8$ ) show weakly unstable CAE mode with  $\omega = 0.4 \omega_{ci}$  and  $\gamma \sim 0.001 \omega_{ci}$ .

- GAE modes are more unstable than CAE (agrees with analytical calculations) with  $\gamma/\omega \sim n_b/n_0$ .
- CAE modes are edge localized, whereas GAE modes are core localized.
- GAE mode have small  $m \sim 1-3$ ; for CAE,  $m \sim 8-10$ .
- GAE mode propagates counter to beam direction.
- Both GAE and CAE modes have large compressional magnetic component near the plasma edge.



$n=4$  ( $m=-2$ )

$n=8$



$n=6$  ( $m=-1$ )



# Resonance condition

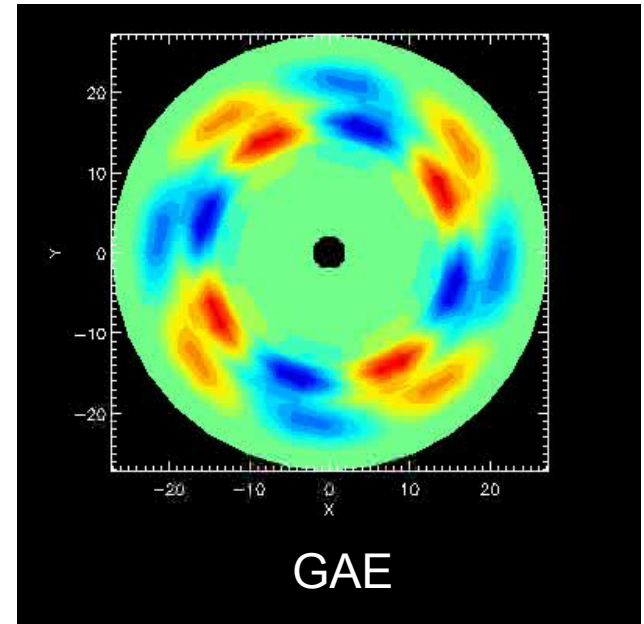
Resonant beam ions satisfy condition:

$$\omega - k_{\parallel} V_{\parallel} - \omega_{ci} \approx 0$$

$$\omega \approx k_{\parallel} V_{\parallel}$$

In the simulations:  $V_{\parallel} > 0$  and  $\omega/k_{\parallel} < 0$ .

For  $\omega = 0.3-0.4\omega_{ci}$  and  $k_{\parallel} V_A \sim 0.3$ , the resonant particles will have  $V_{\parallel} \sim 2V_A \rightarrow$  significant fraction of beam ions can be in resonance.



Contour plot of perturbed fluid pressure at equatorial plane.

# Multiple resonances are seen in particle phase space

## Resonance condition:

$$\omega - l\overline{\omega_{ci}} - \overline{k_{\parallel}v_{\parallel}} - \overline{k_{\perp}v_D} = 0$$

$$\overline{\omega_{ci}} \sim B_0(1 + \varepsilon \cos \theta)$$

$$\overline{k_{\perp}v_D} \sim \sin(\psi + \theta)$$

$$\omega - l\overline{\omega_{ci}} - (nq - m)\overline{v_{\parallel}} / qR - (p + r)\overline{v_{\parallel}} / qR = 0$$

$p, r$  are integers

corresponds to:  $m \rightarrow m' = m - (p + r)$

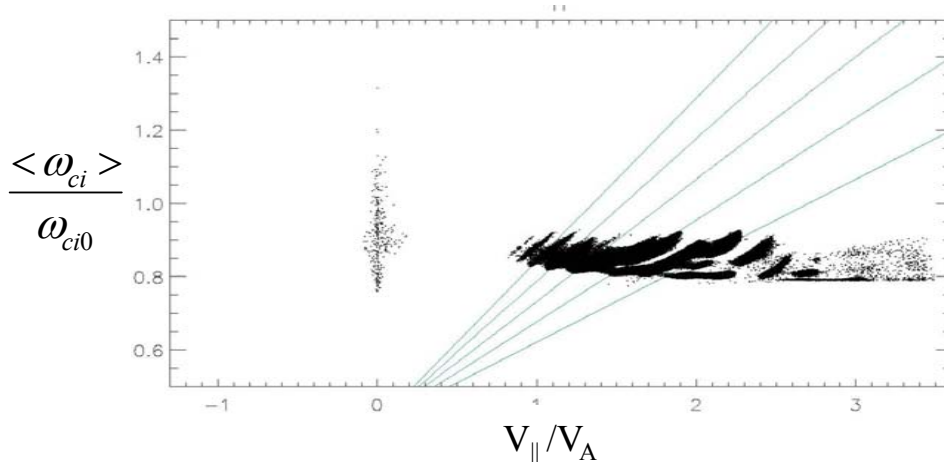
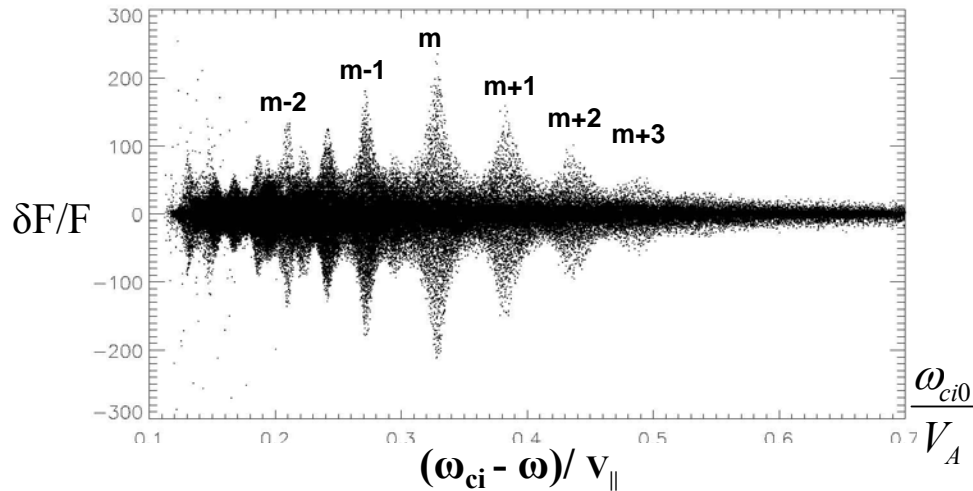


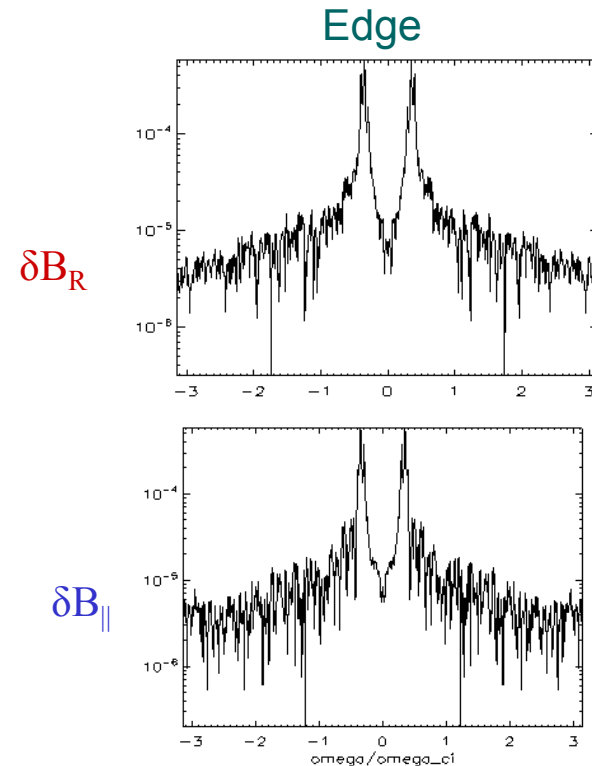
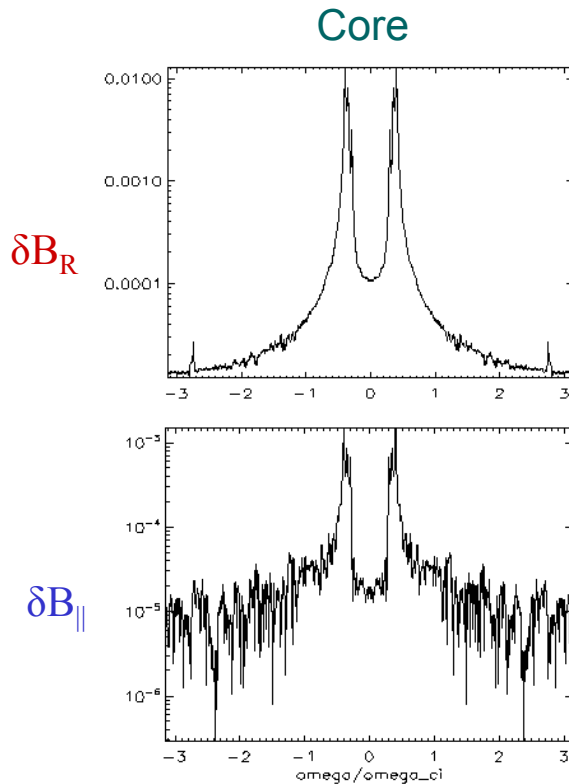
Fig.1 Resonances are shown for one mode with  $\omega=0.4 \omega_{ci}$  ( $m=3$ ). Resonant interaction is seen for  $m; m\pm 1; m\pm 2$  etc

Fig.2 Straight lines correspond to approximate relation:  $\overline{\omega_{ci}} - \omega = \overline{v_{\parallel}} (nq + m') / q_0 R_0$

for  $\omega=0.4$  and  $m'=1-5$ .

Orbit-averaged parallel velocity vs orbit-averaged cyclotron frequency for strongly resonant particles.

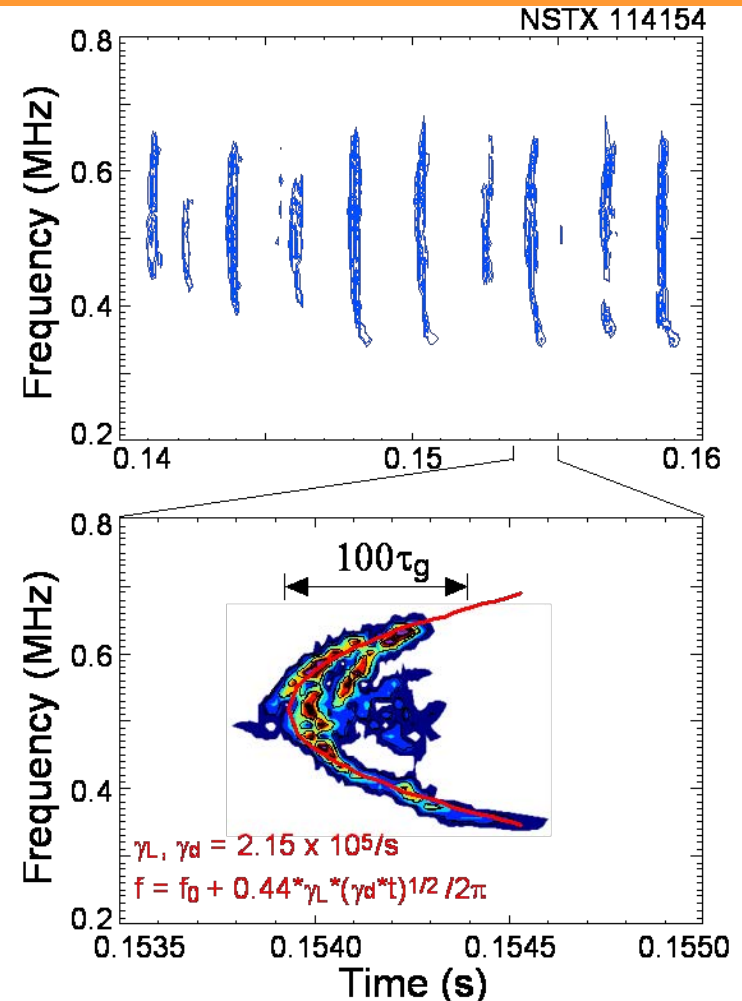
# Magnetic spectrum shows at least three modes with comparable amplitudes



Several modes present with  $\Delta\omega \sim 1/R_0$ :  $\omega=0.3$ ;  $0.35$ ;  $0.4 \omega_{ci}$ .  
Higher frequency mode (higher poloidal mode number  $m$ ) dominates in the core, while lower frequency mode has maximum amplitude at the edge (lower  $m$ ).

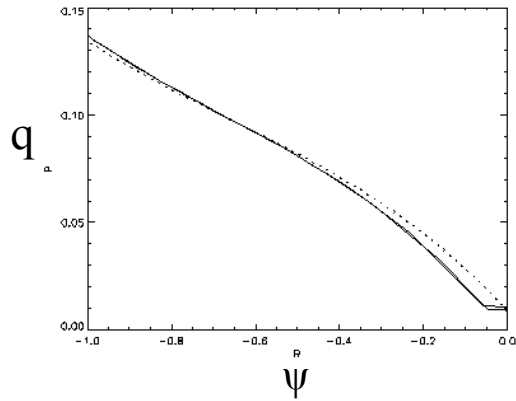
# Most unstable mode in HYM simulations compares well with experimental results for NSTX 114147

- Measured toroidal number  $n=5$  with frequency  $f=480\text{kHz}$  (plasma frame) agrees with simulation results  $f=403\text{-}530\text{kHz}$ .
- Wave propagates opposite to the beam injection direction ie  $\omega/k_{\parallel} < 0$  (GAE mode).
- Linear growth rate is inferred from frequency chirping:  $\gamma \sim 2.15 \times 10^5/\text{s}$  [E. Fredrickson'05 , Berk, IAEA'06 ] compares well with numerically calculated  $\gamma \approx 1.54 \times 10^5/\text{s}$ .

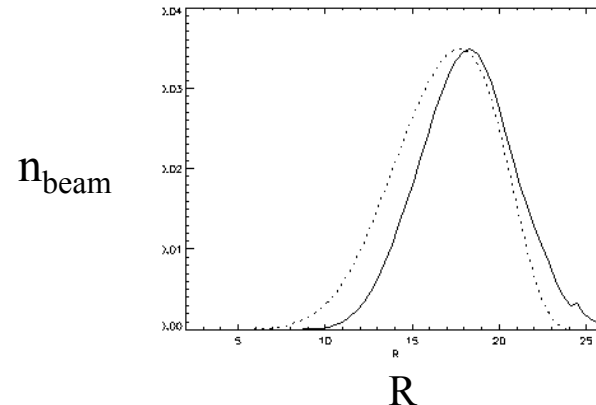


Up and down chirp observed during early NBI on NSTX. [E. Fredrickson, Phys. Plasmas '06].

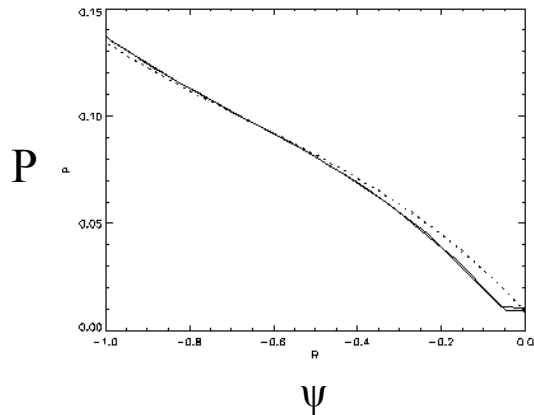
# Plasma parameters and profiles are matched to NSTX shot #114147 (TRANSP)



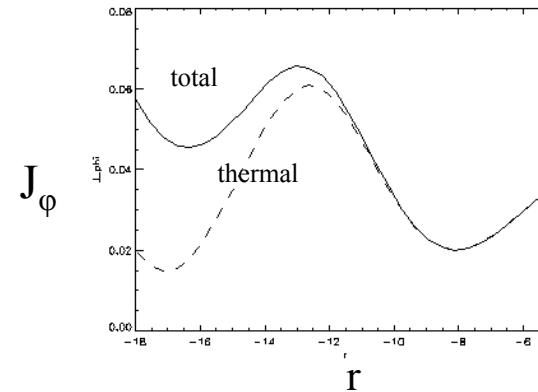
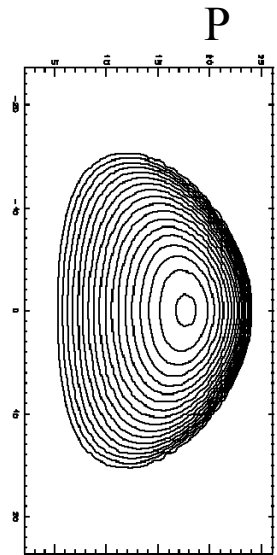
q-profile vs poloidal flux



Beam density vs major radius



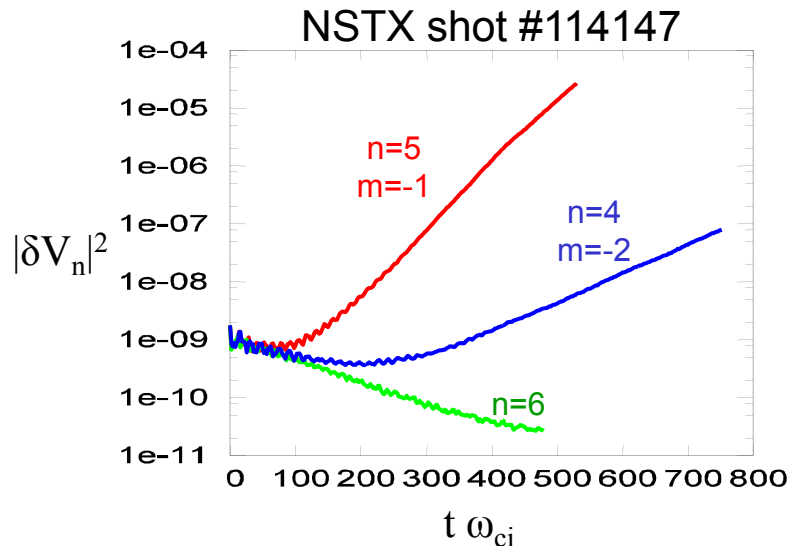
Pressure profile vs poloidal flux



Toroidal current vs minor radius

# Low- $n$ most unstable modes have a character of GAE modes

- Growth rates of unstable modes are very sensitive to details of distribution function (pitch-angle).
- Most unstable mode toroidal number shifts to larger  $n$  for larger  $q_0$ .



$$\gamma_4 = 0.005\omega_{ci} \quad \text{and} \quad \omega = 0.3\omega_{ci}$$

$$\gamma_5 = 0.014\omega_{ci} \quad \omega = 0.3\omega_{ci}$$

$$k_{\parallel} = \frac{\omega_{ci} - |\omega|}{v_{\parallel}}$$

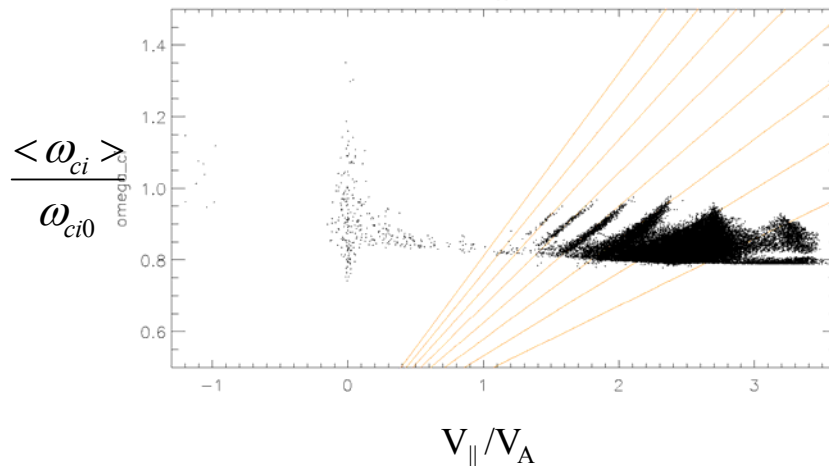
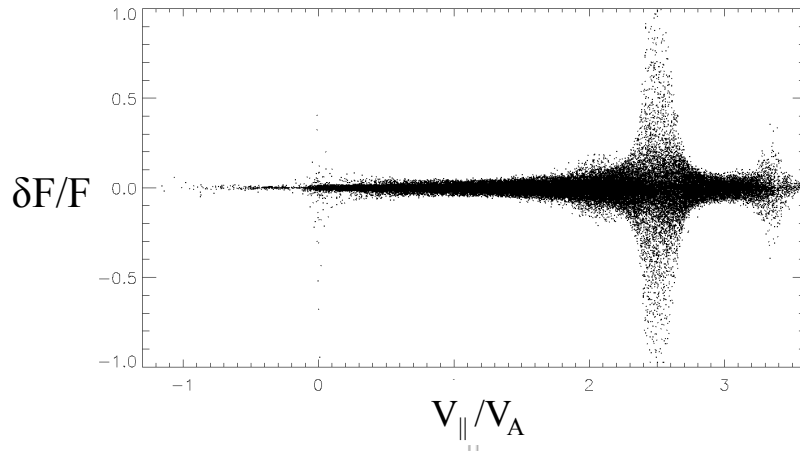
Observed features agree with that of GAE mode, which exists just below the lower edge of the Alfvén continuum:

- For each  $n$ , several  $m$  are unstable with large  $k_{\parallel}$  and  $nm < 0$ .
- Localized near magnetic axis.
- Large  $\delta B_{\perp}$  component in the core.

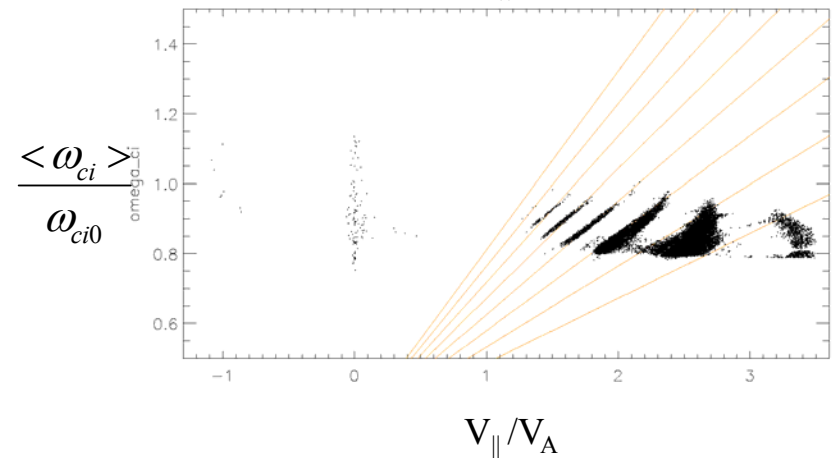
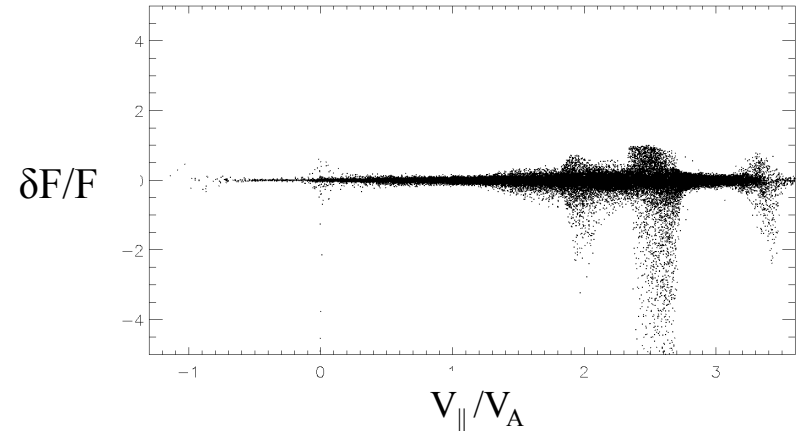
- Main damping mechanism for GAE is continuum damping (modeled in HYM with artificial viscosity):  $\gamma_d/\omega \sim (r/r_{res})^{2m+\delta}$
- Modes with larger- $m$  have smaller radial extent.

# Location of resonant particles in phase-space

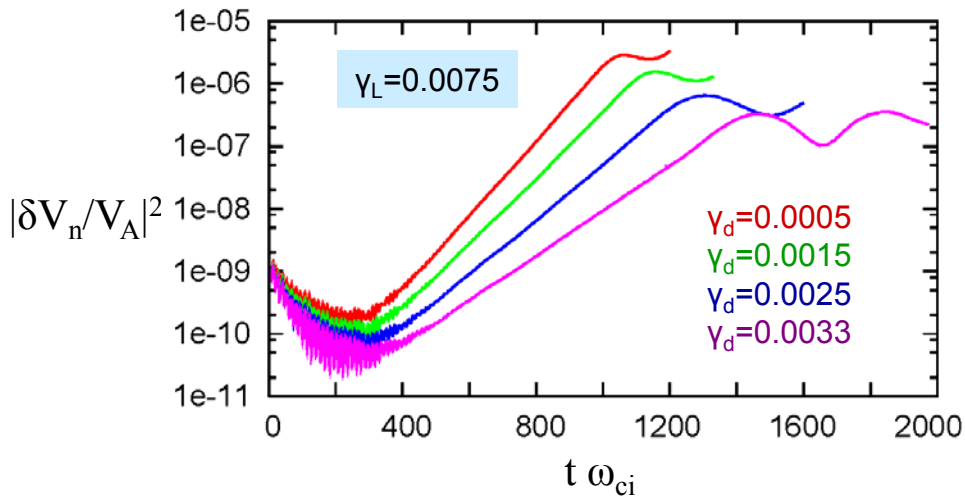
Linearized simulations



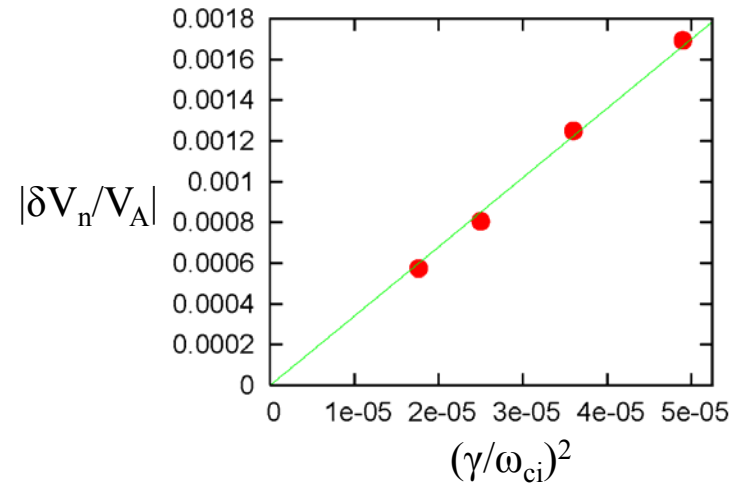
Nonlinear simulations



# Simulations show nonlinear saturation of GAEs due to particle trapping



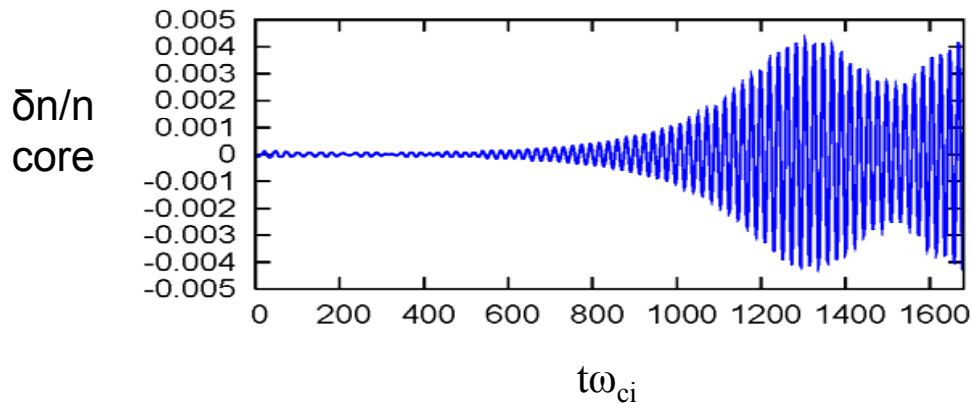
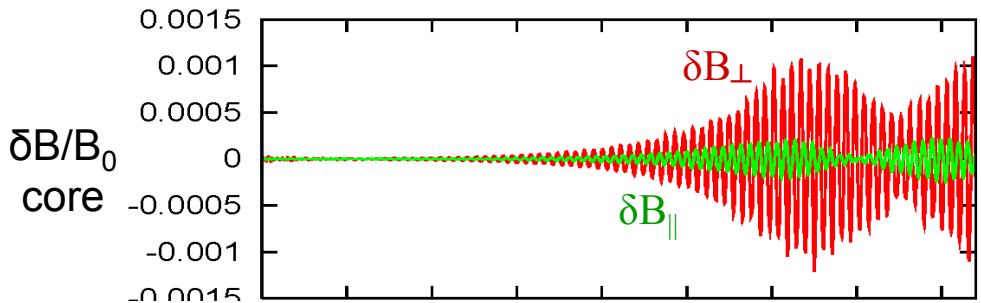
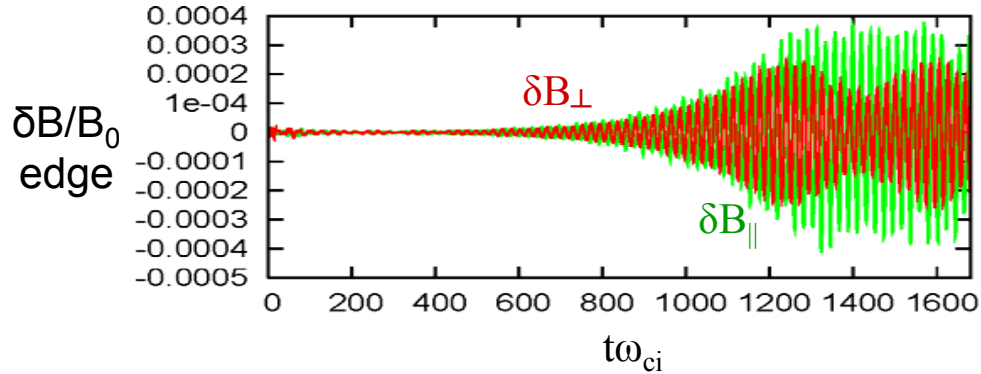
Time evolution of kinetic energy from four nonlinear simulations with different damping parameter.



Saturation amplitude vs  $\gamma^2$  ( $n=4$ ,  $m=-2$ ).



# Magnetic field and density perturbations



Simulations with  $n=4$   $m=-2$

$$\gamma = 0.005\omega_{ci} \text{ and } \omega = 0.3\omega_{ci}$$

$$\gamma_L = 0.0075\omega_{ci}; \quad \gamma_d = 0.0025\omega_{ci}$$

At peak amplitude  $\delta B_{\parallel} < 1/3 \delta B_{\perp}$ ;  
at the edge the compressional  
component dominates  $\delta B_{\parallel} > \delta B_{\perp}$ .

## Experimental measurements:

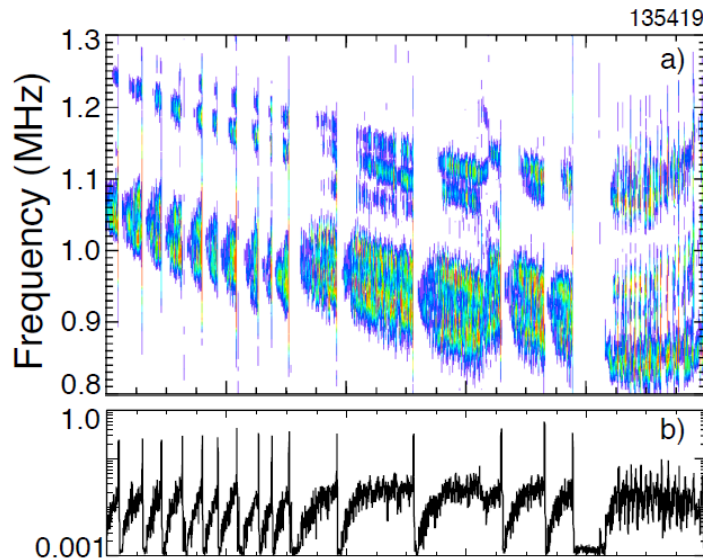
$\delta B_{\parallel} > \delta B_{\perp} \sim 10^{-4} B_0$  (at the edge),  
 $\langle \delta n \rangle / \langle n_0 \rangle \sim 10^{-4}$ .

Taking into account mode localization  
and time-averaging, for peak  
amplitude:  $\delta n \sim 3 \cdot 10^{-3} n_0$

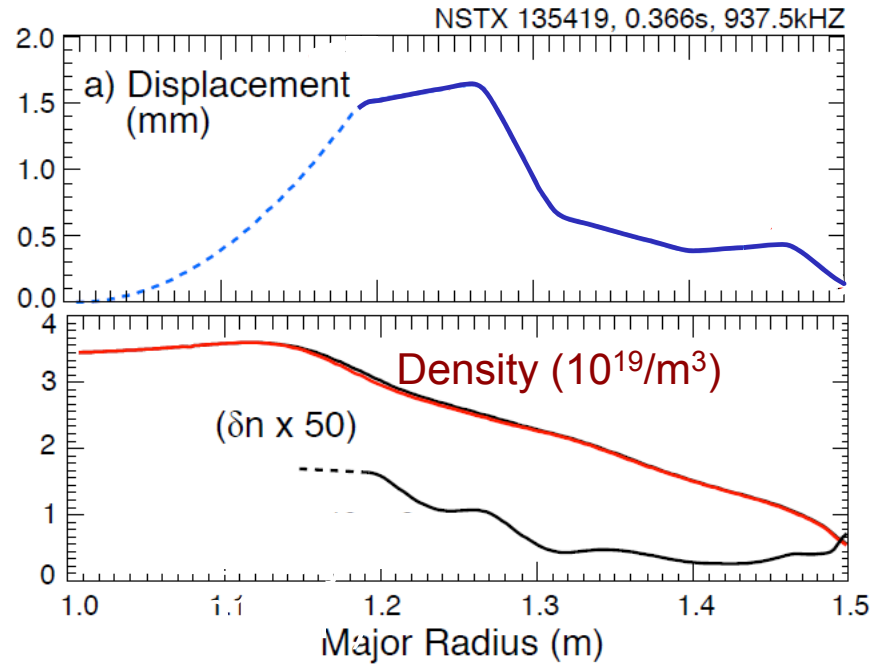
GAE bursts can have amplitude much  
larger than time-averaged, with peak  
amplitudes  $\delta n \sim 10^{-2} n_0$ .

# Observation of Global Alfvén Eigenmodes in NSTX

[E. Fredrickson et al, IAEA 2010]



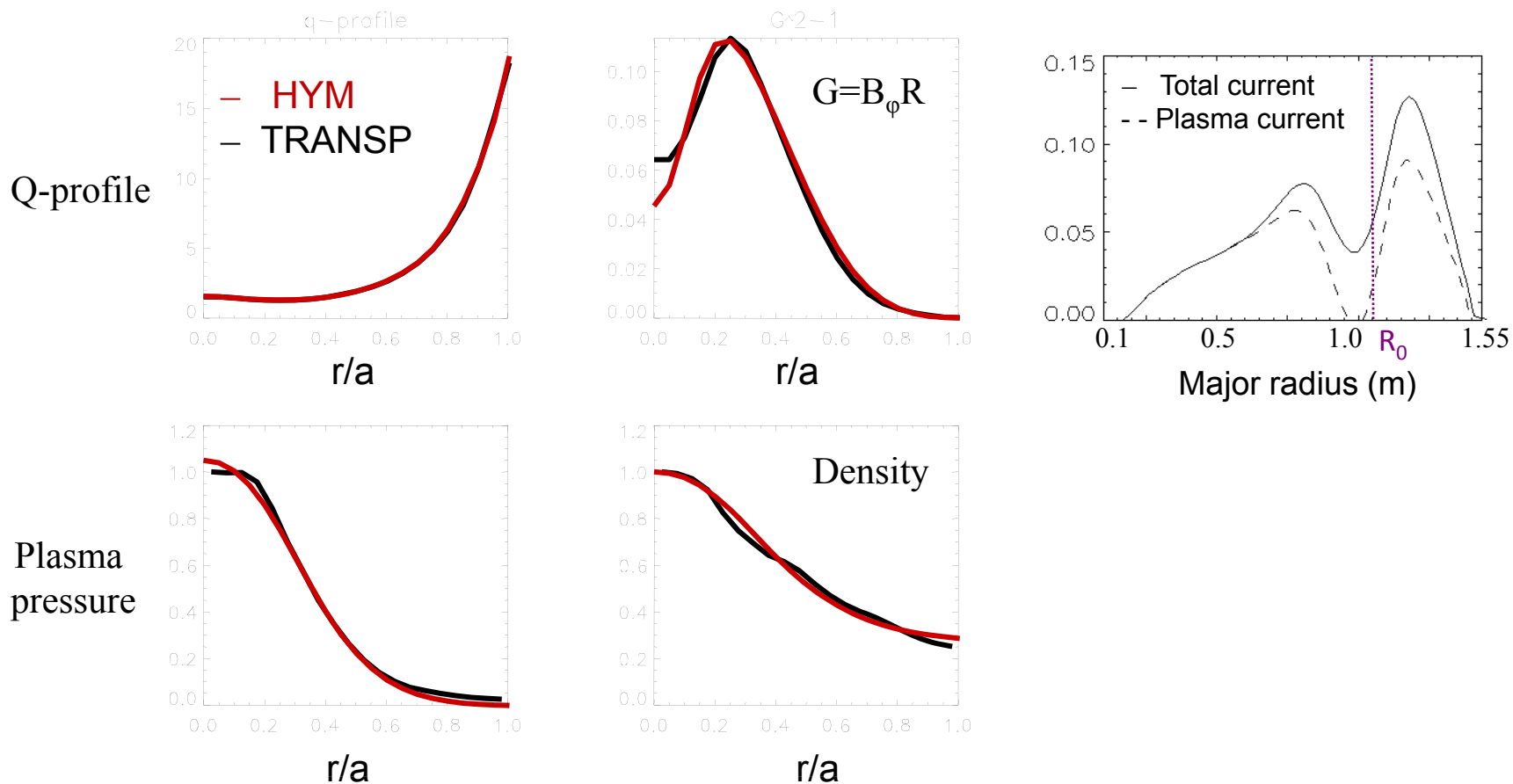
(a) Spectrogram showing GAE modes,  
 (b) magnetic fluctuations  $0.8\text{MHz} < \text{freq} < 1.3\text{MHz}$



a) Mode amplitude profile.  
 b) Density profile and perturbed density.

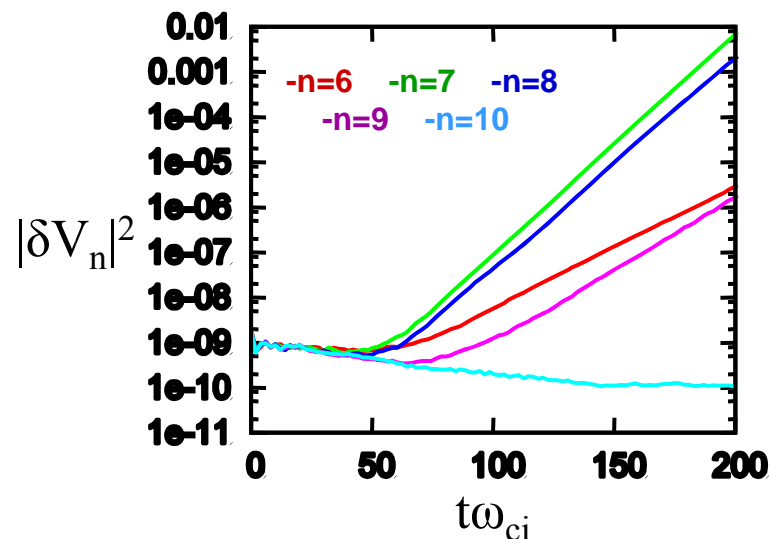
At the edge the compressional component dominates  $\delta B_{\parallel} > \delta B_{\perp}$ ,  $\delta n \sim 10^{-2} n_0$ .

# Plasma parameters and profiles are matched to NSTX shot #135419

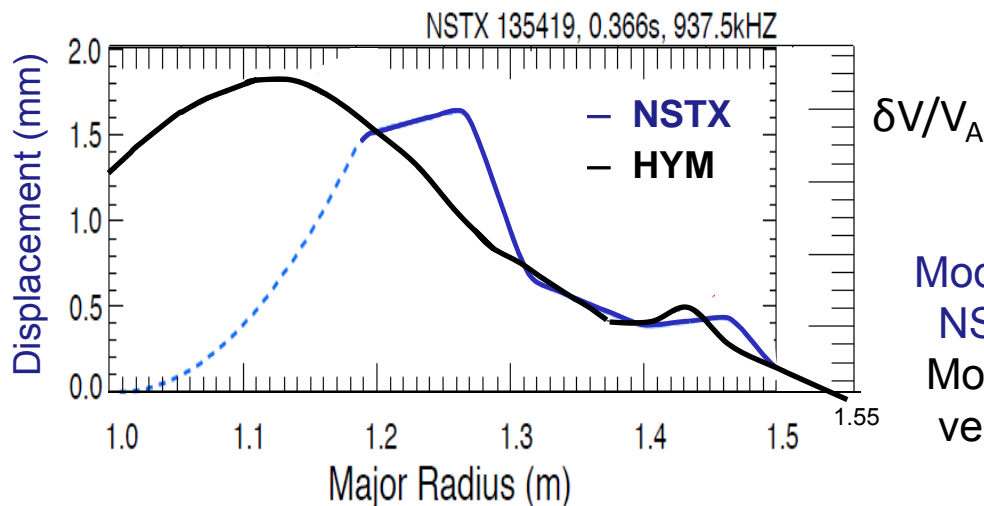


# HYM simulations comparison with experimental results for NSTX shot#135419

- Several modes are unstable with toroidal mode numbers  $n=6 - 9$  and frequencies  $f=0.4-0.8\text{MHz}$  (plasma frame) compared to experimental results of  $n=7 - 11$ , and  $f=0.8-1\text{MHz}$ .
- GAE modes.
- Similar mode structure.



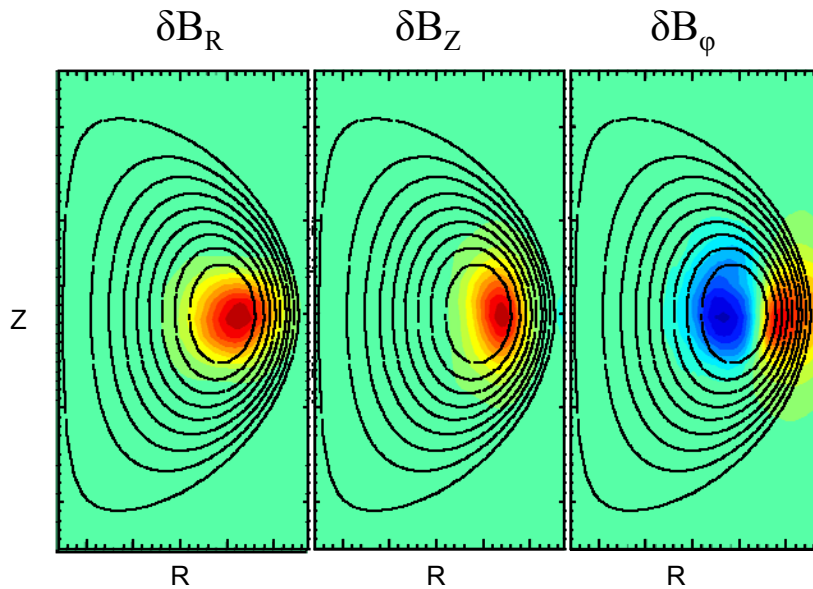
Time evolution of kinetic energy from linearized simulations with  $n=6-10$ .



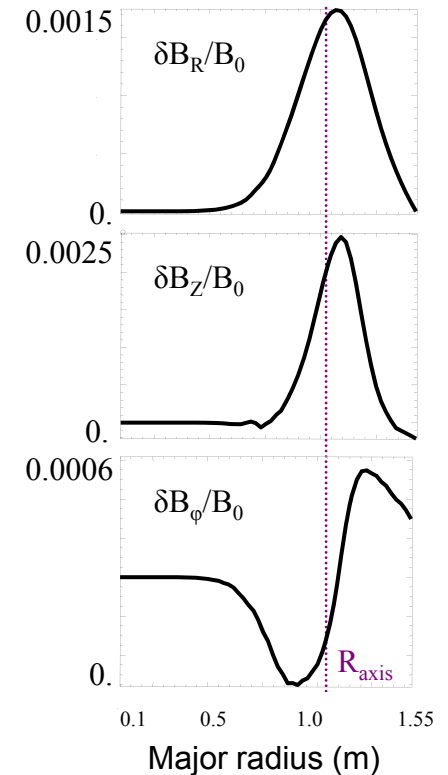
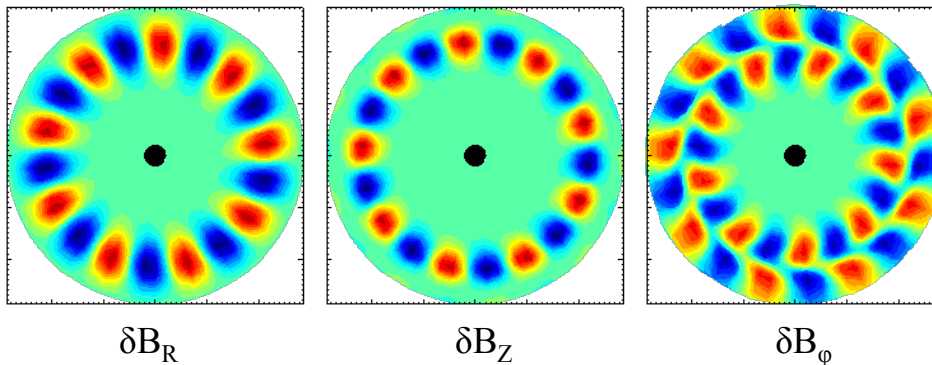
Mode amplitude profile - displacement NSTX#135419 [E. Fredrickson, IAEA 2010]. Mode structure from HYM simulations – velocity profile for  $n=9$ .

# Mode structure: magnetic field (n=9)

GAE modes always have significant compressional component at the edge



- $\delta B_{\parallel}$  is small near magnetic axis, but it is peaked at low-field side mostly due to large  $\delta B_Z$ .
- Phase relations between  $\delta B$  components are consistent for all R.
- $\delta B_{\parallel}$  is large at the edge due to wide radial profile of  $\delta B_{\phi}$ .



Radial profiles of perturbed magnetic field at the midplane.

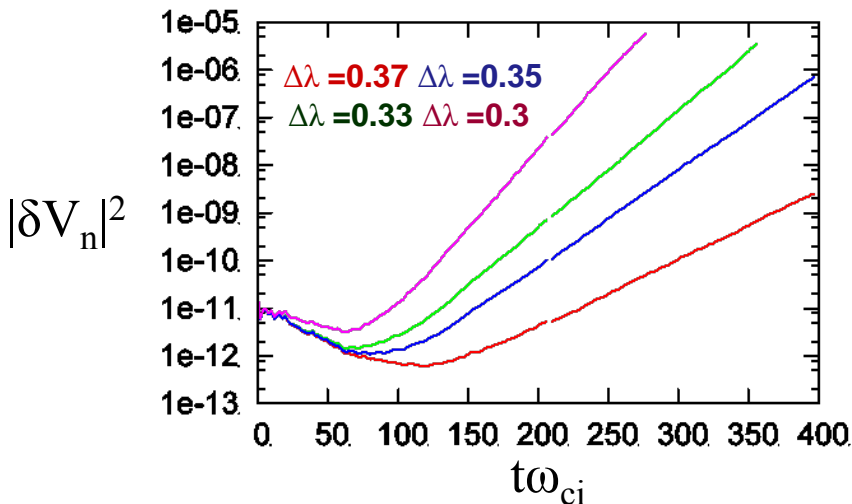
# Driving mechanism for GAE modes (n=9)

Delta-f model allows detailed analysis of the instability drive:

$$w = \frac{\delta f}{f}, \quad f = f_0 + \delta f$$

$$\frac{d}{dt} \delta f = -\frac{d}{dt} f_0 = \underbrace{-\frac{d\varepsilon}{dt} \frac{\partial f_0}{\partial \varepsilon}}_{\text{stabilizing}} - \underbrace{\frac{dp_\phi}{dt} \frac{\partial f_0}{\partial p_\phi}}_{\text{stabilizing}} - \underbrace{\frac{d\lambda}{dt} \frac{\partial f_0}{\partial \lambda}}_{\text{destabilizing - responsible for instability}}$$

stabilizing    stabilizing    **destabilizing –  
responsible for  
instability**



Pitch angle distribution has strong effect on the GAE growth rate:

$$f_0 \sim \exp[-(\lambda - \lambda_0)^2 / \Delta\lambda^2]$$

$$\lambda = \mu B_0 / \varepsilon$$

# Conclusions

---

- Self-consistent simulations using the HYM code show that for large injection velocities, and strong anisotropy in the pitch-angle distribution, many Alfvén modes can be excited by NBI ions.
- Sub-cyclotron frequency modes are driven unstable via Doppler-shifted cyclotron resonance.
- Multiple fast ion resonances are seen for each mode (poloidal mode number).
- Magnetic mode structure for GAE in NSTX shows significant compressional component at the edge.
- Simulations show nonlinear saturation of GAEs due to particle trapping.
- Saturation amplitudes and mode structure are comparable with the experimental measurements.
- Drift-kinetic electron model has been implemented in the HYM code, and it will be used to study the effects of GAE modes on the electron transport.